Origin of Septarian Concretions in the Huron Member of the Ohio Shale (Devonian), Delaware County, Ohio

Senior Thesis

Submitted in partial fulfillment of the requirements for the

Bachelor of Science Degree

At The Ohio State University

By

Jacob Meyer

The Ohio State University

2019

Approved by

Loren E. Babcock, Advisor
School of Earth Sciences

TABLE OF CONTENTS

Abstract

One of the lesser understood features of concretions is a variety of heavily fractured concretions, named septarian concretions. By taking a new approach in the study of septarian fracture patterns, it is possible to connect the episode of fracturing to a wider tectonic event and better understand how and when they fractured. In March 2019, such a study was performed on the septarian concretions of Shale Hollow Park in Columbus, Ohio. The pattern of their fractures as well as observations made on the surrounding shale unit suggest the presence of two fracturing episodes. One episode appears in the concretions but fractures in the surrounding shale lack the pattern, suggesting the first episode of fracturing occurred after concretion formation but before the lithification of the surrounding shale. If the concretion was formed and brittle enough for tensile failure while the surrounding shale was not, this has implications for the time required to form a concretion. Contrary to the traditional view on concretion formation, this suggests that concretions formed synsedimentary. The second episode of fracturing is reflected in the joints of the surrounding shale and fractures that only pierced the outer ring of the concretions. This suggests a possible compositional similarity between the shale and the outer ring of the concretions. These conclusions could be tested by similar studies of septarian concretions in the corresponding Upper Devonian black shales in other localities. A geochemical analysis of the outer rings could prove insightful too.

Acknowledgments

First, I would like to thank my family, starting with my maternal grandmother, Beckey Molloy. You've always had a special role in my life. Even when I forget to respond to your text messages. Next are my supportive parents, Joseph and Leslie Meyer. You guys have stuck by me through it all and I can't thank you enough for that. To my sisters, Claire and Emma: thank you both for offering a different point of view as we grew up. To our faithful dog, Sonny: thank you for always being a good boy.

Next, I would like to thank my peers and the faculty within the School of Earth Sciences. I was nervous when I changed majors during my sophomore year, but the friendly and energetic people within SES helped me find my place here. First of all, I would like to thank the faculty as a whole. Since coming to the SES, I've yet to take a class where the professor wasn't excited about the subject matter and excited about teaching it. The energy that they bring into their lectures is truly inspiring. In particular, I'd like to thank Dr. Michael Barton, Dale Gnidovec, Dr. David Young, Dr. Ashley Griffith, Dr. Michael Bevis, and Dr. Lawrence Krissek. I would also like to thank my research advisor, Dr. Loren Babcock. In addition to faculty, I would like to thank my friends and classmates in SES. Whether it's scrambling to finish a lab assignment or scrambling up an outcrop, I genuinely appreciate and enjoy working and talking with all of you. On the topic of outcrops, I never could have experienced the outcrops of central Utah if it wasn't for two scholarships. I would like to thank the donors of the the School of Earth Sciences Field Experience Travel Fund and the Edmund M. Spieker Memorial Scholarship.

List of Figures

List of Tables

INTRODUCTION

Septarian concretions are concretions that have undergone extensive fracturing. Despite the considerable level of fracturing, septarian concretions tend to have the same spherical or spheroid shape consistent with other concretions. There is considerable variance in the size of septarian concretions. Regardless of size, the fractures tend to be splayed across the concretion, similar to the pattern of spokes on a wheel.

Concretions form as a result of the decay of recently buried, organic material in an aquatic environment (Borkow and Babcock, 2003). In an aquatic environment, a three-dimensional array of fungus and bacteria envelop a recently deceased organism (Borkow and Babcock, 2003). Borkow and Babcock refer to this structure as a microbial halo and it is interpreted to be the precursor to a concretion (2003). Depending on the stability of the halo, the chemical conditions within the halo could be favorable for mineral deposition (Borkow and Babcock, 2003).

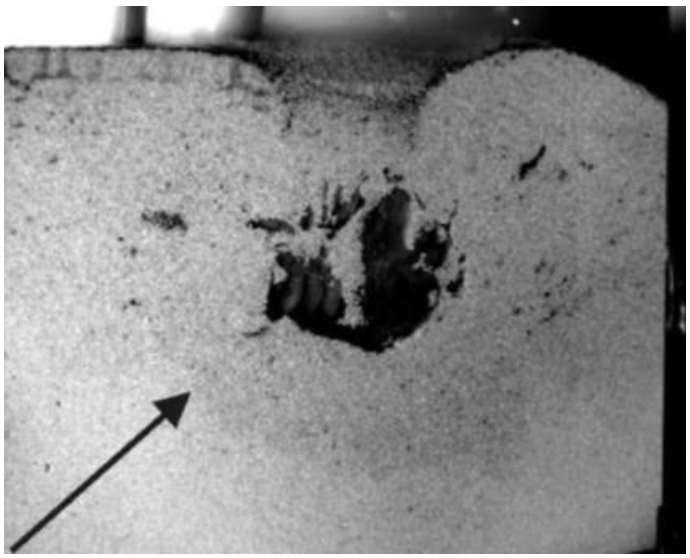

Figure 1. Horseshoe crab (Limulus) decaying in sand and surrounded by and surrounded by dark bacterial-fungal halo (arrow). Length of halo approximately 8 cm. Reprinted from “Turning Pyrite Concretions Outside-In: Role of Biofilms in Pyritization of Fossils” by Borkow and Babcock, 2003, *The Sedimentary Record*, *1*, 5. Copyright 2003 by the Society for Sedimentary Geology. Reprinted with permission.

For the purposes of this analysis, it is useful to separate the interior of the large carbonate concretion into concentric zones called rings. The concretions can be divided into three rings. Many of the concretions had an area at their center that was completely eroded. This area is the first ring. In other concretions, the central area appeared to contain barite. For those concretions with preserved barite, the outer edge of the first ring is the last occurrence of barite crystals. The second ring includes all material from the outer edge of the first ring to a ring of shale. Some of the concretions did not have any preserved carbonate outside of this ring of shale.

Large carbonate concretions are a persistent feature in the Huron Shale Member of the Ohio Shale in Ohio (Hellstrom and Babcock, 2000). They are present in numerous outcrops at the surface in central Ohio. The carbonate concretions occur in large numbers along distinct horizons (H&B). In places, some of the concretions have a septarian morphology. Work to understand the origin and development of these concretions is in progress. In this thesis, I discuss evidence for the timing of cracks in large carbonate concretions from the Huron Member in an extensive exposure in southern Delaware County, Ohio. Evidence suggests that two phases of crack development took place. One phase was synsedimentary and may have been associated with tectonic activity related to development of the Appalachian Foreland Basin, and a later phase was evidently related to the same stresses that resulted in the formation of joints in surrounding shales.

Figure 2. Septarian concretions at Shale Hollow Park. The septarian style fractures can be seen passing through the central ring and, in most cases, penetrating the layers on the other side. One concretion has its central ring preserved (right) and the central ring of the other concretion has eroded (top left and bottom left). In both left images, the three rings are visible.

Location and Geologic Setting

Location

Shale Hollow Park was selected for study because of expansive exposure of the Huron Member of the Ohio Shale and abundance of carbonate concretions. At the time of this work, more than a dozen concretions were sufficiently exposed that they could be studied, all displaying septarian pattern fracture. The park is easily accessible and open every day of the week between 8 a.m. and 9 p.m.

Figure 3. Map of Ohio from Google Maps, with Shale Hollow Park labeled.

Geologic Setting

The Huron Shale Member of the Ohio Shale. The Ohio Shale is an Upper Devonian unit. The Huron Member consists of organic-rich, laminated, black shales with a few intervals and gray mudrock layers (Hellstrom and Babcock, 2000). The unit varies between 40 m and 50 m in thickness throughout its occurrence in central Ohio (Hellstrom and Babcock, 2000). Carbonate concretions occur throughout the lower 25 m of the unit across discrete horizons (Hellstrom and Babcock, 2000). The concretions vary in size, some growing up to 3 m in diameter and others only growing to 45 cm in diameter (Hellstrom and Babcock, 2000).

The Ohio Shale was deposited as a distal of the Appalachian Basin (Hellstrom and Babcock, 2000). The Appalachian Basin, a foreland basin, formed because of isostatic downwarping associated with the Acadian orogenic event (Hellstrom and Babcock, 2000). The Acadian Mountains served as a source of siliciclastic sediments that were deposited in the basin

(Hellstrom and Babcock, 2000). Given its distal location and the clinoform structure associated with foreland basins, the Ohio Shale is interpreted to have been deposited in a deep water basin.

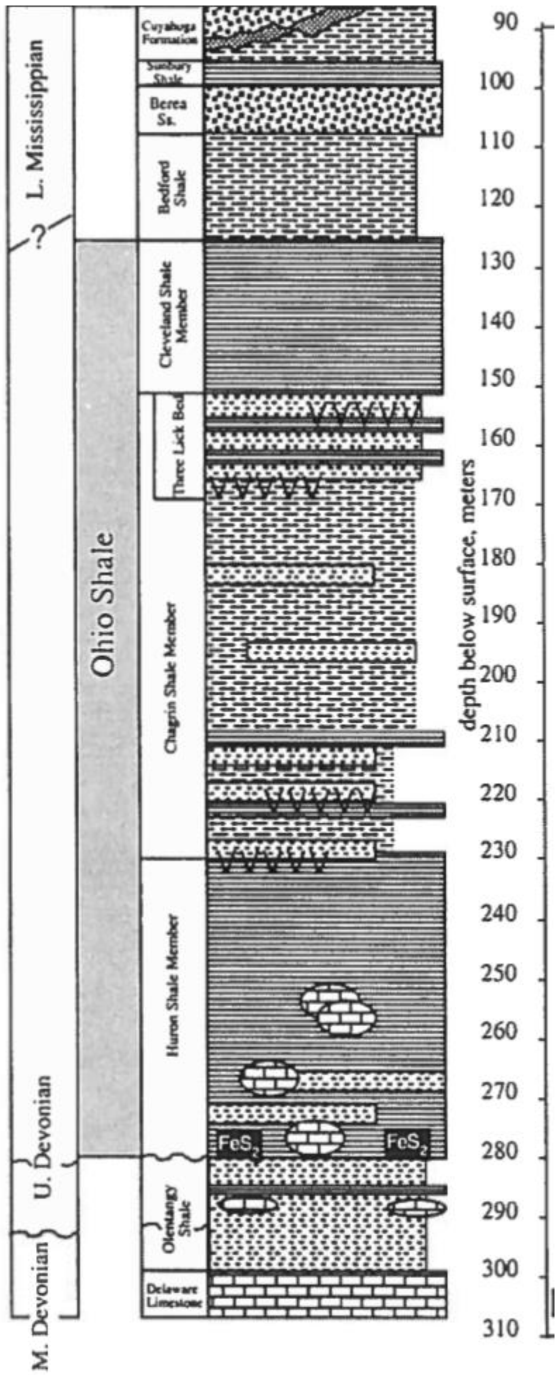

Figure 4. Stratigraphic column. The concretions used in this study occur in the limestone horizon near 270 m below surface. Adapted from “High-Resolution Stratigraphy of the Ohio Shale (Upper Devonian), Central Ohio” by Hellstrom and Babcock, 2000, *Northeastern Geology and Environmental Sciences, 22,* 207. Copyright 2000 by Northeastern Geology and Environmental Sciences. Adapted with permission.

METHODS

The concretions used in the study occur in the Huron Member of the Ohio Shale. Measurements of strike were taken on cracks expressed within septarian concretions cropping out in Shale Hollow Park, Lewis Center, Ohio.

Field Tests

The strike of cracks in septarian concretions were measured during March 2019. Using the iPhone default compass app or a Brunton compass with 4.5-degree correction, the trends of concretion fractures were taken as well as noting the number of rings in the concretion and which rings the fracture penetrated. As the fractures were roughly vertical, they were treated as linear features along the exposed sides of the concretion. Trends measured were taken pointing towards the center of the concretion. In addition to fractures within the concretions, prevalent shale jointing directions were measured with the same measuring tools as the concretion fractures. The measurements of the fractures were recorded as well as noting how many rings the concretion had. Using Microsoft Excel, rose diagrams were created to plot the fracture trends. The rose diagrams were created with radar plots with a bin size of 10 degrees. One rose diagram for each individual concretion was created as well as one rose diagram for the whole data set, the fractures that only penetrated the outermost ring, the fractures in two-ring concretions, and the fractures in three-ring concretions.

The concretions were found to show two or three concentric zones or “rings.” In septarian concretions having two rings, cracks penetrated both rings. In septarian concretions having three rings, one set of cracks penetrated the all the rings, and another set of cracks penetrated only the outer ring. All sets of cracks were measured. In addition, joint directions in the black shale were measured.

3D Model Analysis

In this analysis, a 3D model of the surface of a septarian concretion was created using a stereophotogrammetric technique of structure from motion. Photogrammetry is a method of making measurements from photographs. In its earliest form, it involved measuring the distance between two points on a photograph. Stereophotogrammetry involves calculating three dimensional coordinates of an object using multiple photographs of the object taken from different views. The model was created by using Agisoft to scan a series of photographs of the concretion. I then wrote a MATLAB script that imports data from the model and replicates the 3D surface based on curvature. The program reads in the model’s coordinate data and calculates curvature throughout the surface. It creates a surface plots reproduction of the model that tracks mean curvature through color, using the curvature and coordinate data.

Several third-party functions were used in the making of the plots. STLRead was needed to import numerical data from the STL file of the Agisoft model. It saves the vertices, faces, and face normal vectors of the model as a fv structure, so that the patch() function, built into MATLAB, can create plots of the data. PatchCurvature was needed to calculate the curvature. Its inputs are the fv structure and true or false, depending on whether the user wants to restrict calculations to third order neighboring vertices. Its outputs are Gaussian curvature, mean curvature, direction of the first principal curvature component, direction of the second principal curvature component, magnitude of the first principal curvature component, and magnitude of the second principal curvature component. Gaussian curvature is the product of the first and second principal curvature components at a given point, while the mean curvature is the average of the principal curvature component. Each principal component represents the maximum and minimum values of curvature along a plane cutting through a 3D surface. So the principal curvature components represent the two planes cutting a surface at a particular point whose cross sections of the surface have the highest and lowest curvature respectively. I made two plots, one with Gaussian curvature represented as color and one with mean curvature represented as color.

The curvature plots and the Agisoft model were qualitatively compared side-by-side, paying attention to fractures on the Agisoft model where local peaks and troughs on the curvature plot occurred. The interaction between Gaussian and mean curvature was also considered. As, explained in Figure 1, the signs of both types of curvature can create very different shapes for the surface.

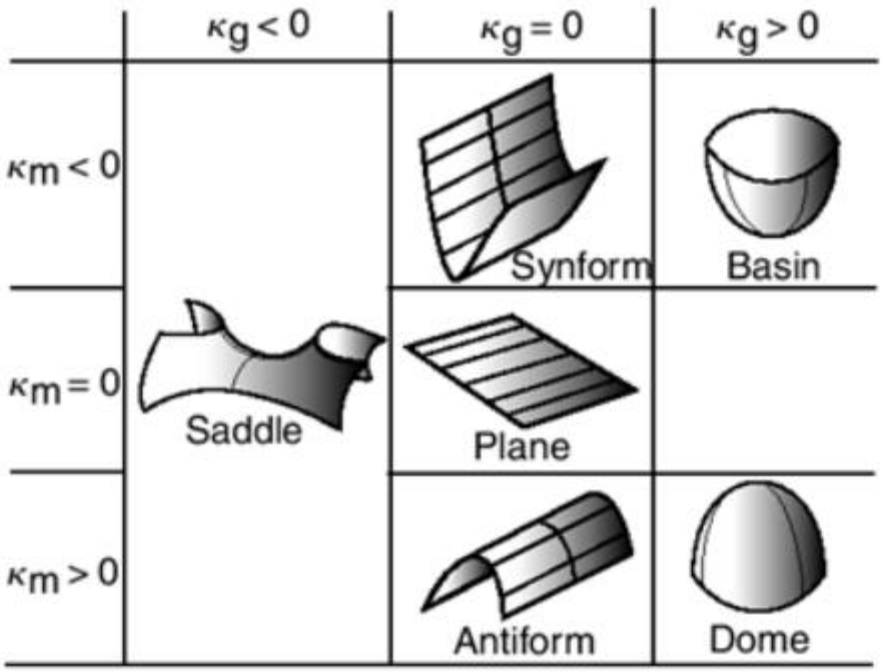

Figure 5. What this is. Km is mean curvature, Kg is Gaussian curvature. The figure shows common shapes associated with a mean and Gaussian curvature of the sign in the table, at an arbitrary point (Pollard and Fletcher, 2005).

Results

Fracture Pattern Analysis

In total, 56 fractures were measured from 14 concretions. There was an even split between two-ring and three-ring concretion fractures. The most common trend among all fractures was in the bin 240-249 degrees, roughly southwest-northeast trending, and 340-349 degrees, nearing north-south trending.

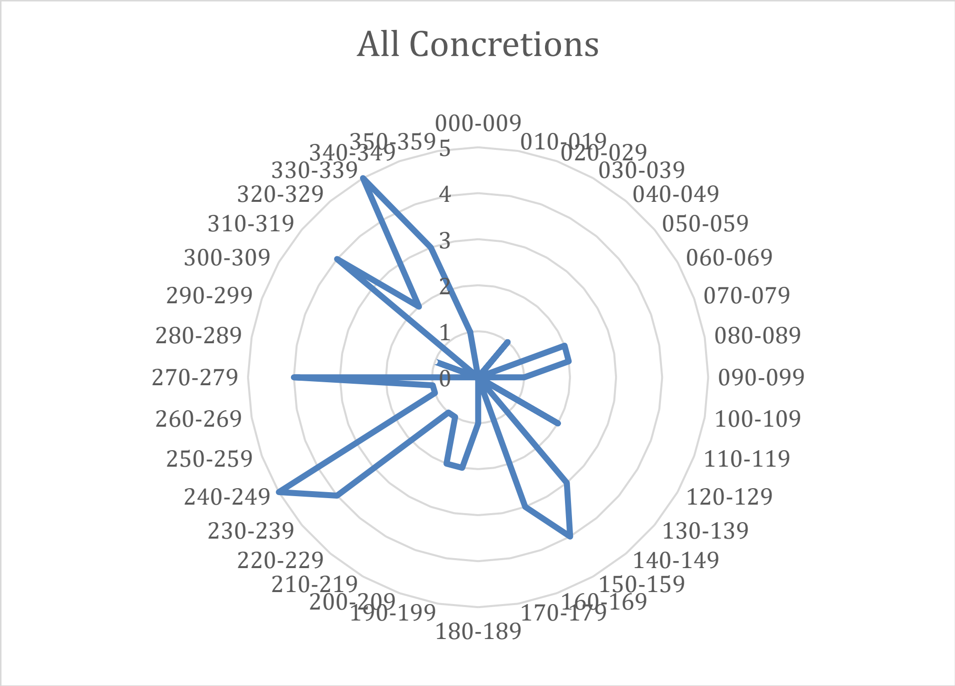

Figure 6. Rose diagram including fracture measurements from all the concretions in the study.

Among the two-ring concretions, the bin with the most fractures was the 340-349 range and among the three-ring concretions, the 160-169 degree bin held the most fractures. Among fractures that only penetrated the outermost ring, the 310-319 bin and the 270-279 bins held the most fractures.

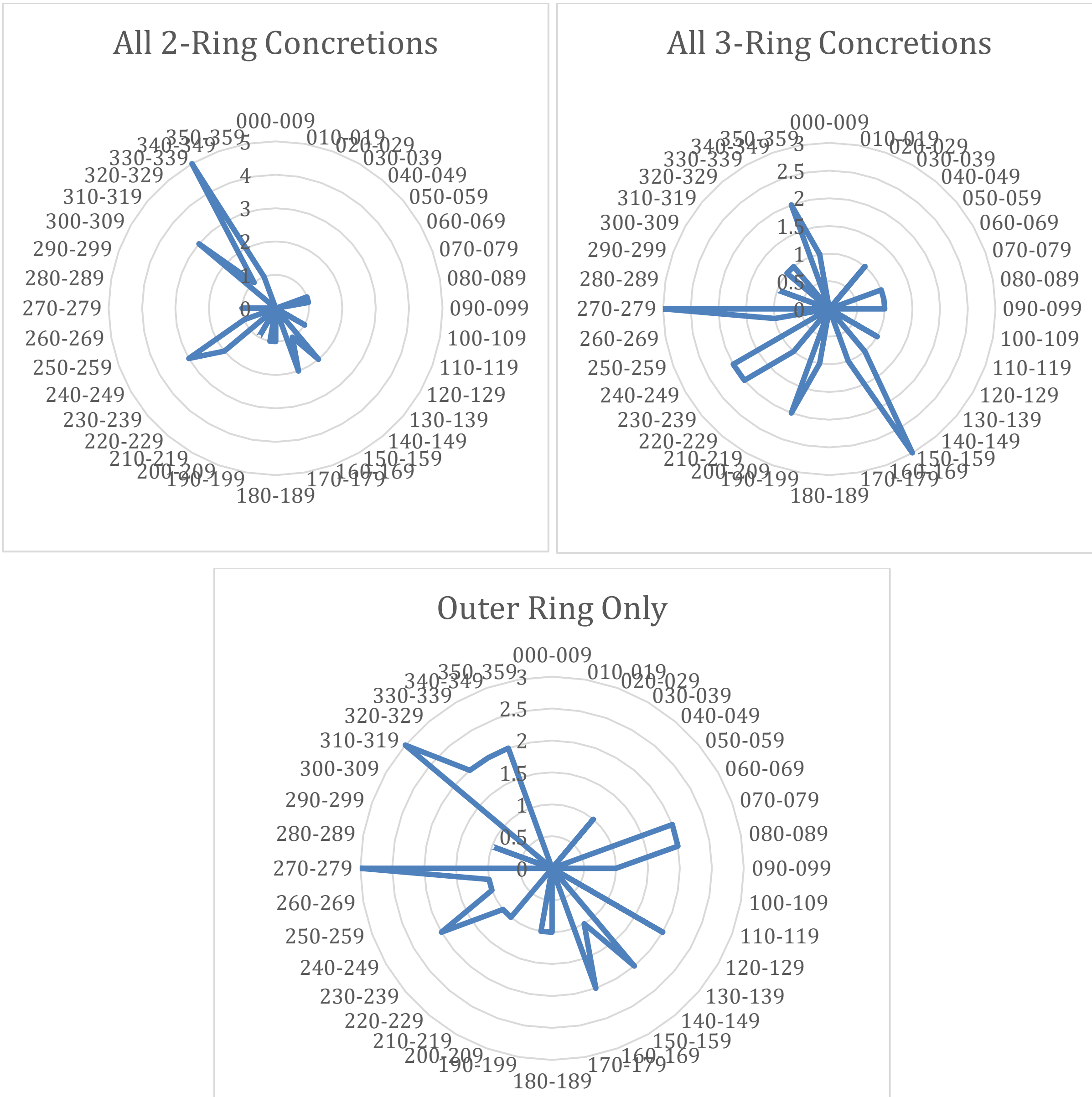

Figure 7. Rose diagrams plotting the trends of fractures in two-ring concretions (top left), three-ring concretions (top right), and fractures that only penetrated the outermost ring.

In addition to concretion fractures, the joint directions in the surrounding shale were measured. The joints were plotted using Almendinger's free stereonet software and on a rose diagram.

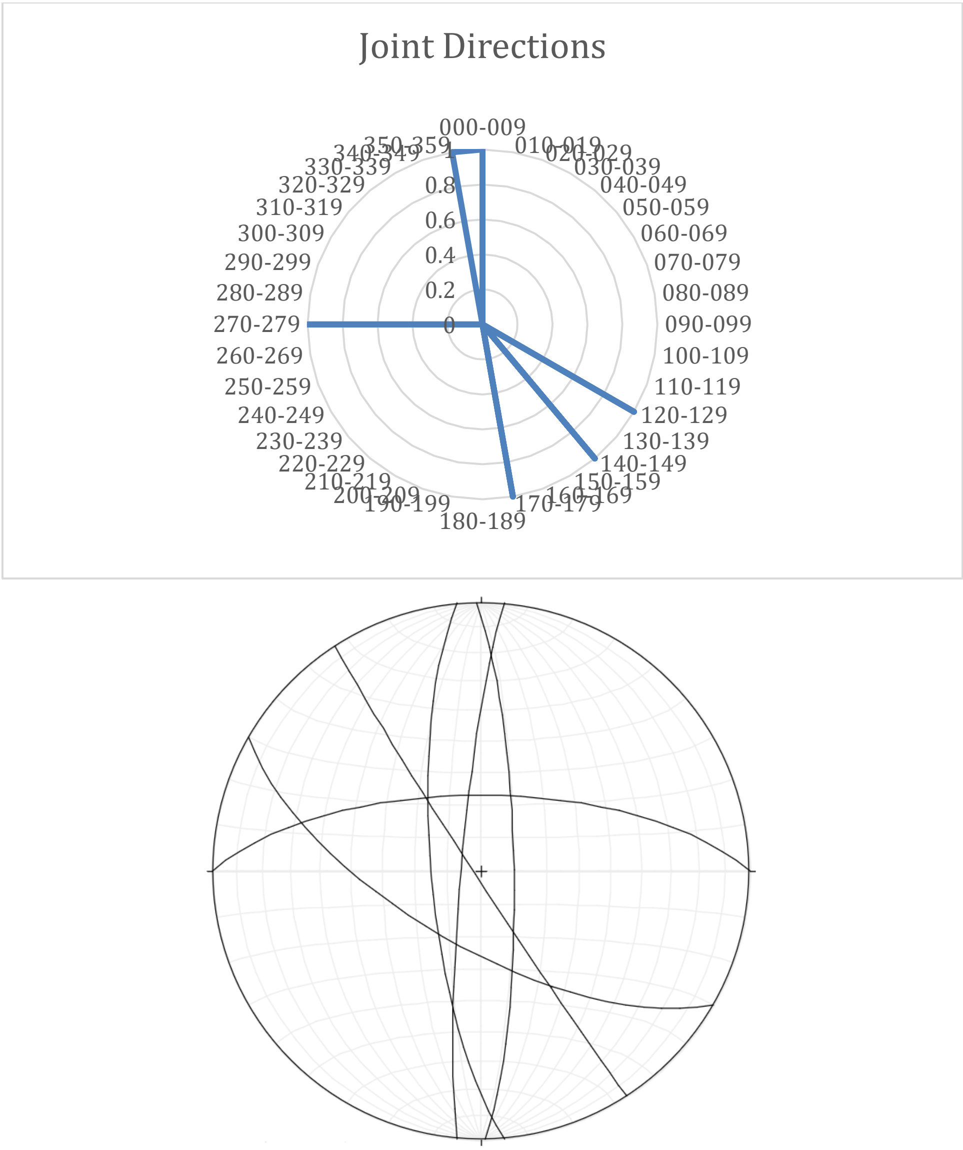

Figure 8. Rose diagram (top) and stereonet (bottom) of the joint directions in the surrounding shale.

Shale Joints		
Strike	Dip	Dip Direction
270	67	N
5	84	W
175	75	W
147	88	W
120	67	SW
359	80	E

Table 1: Table of values corresponding to the orientation of the shale joints measured at Shale Hollow Park.

3D Model Analysis

The magnitude of mean curvature throughout the surface ranges from near zero, orders of magnitude as low as negative fifteen, to 0.5. Overall, there is not a stark change in curvature until the lip of the "top" side. However, there is an area near one end of the concretion's long axis with mean curvature values around 0.5 and contains four outward, radial fractures. The center of the surface contains mean curvature values close to 0, but also contains gaussian curvature values frequently change from positive to negative from point to point.

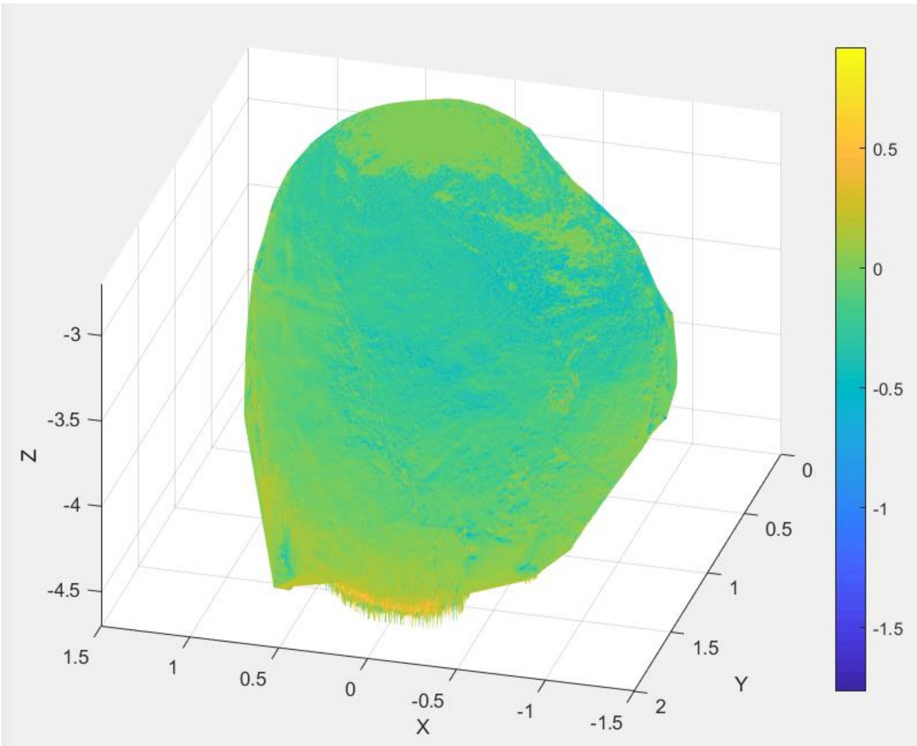

Figure 9: Mean curvature plotted by the color scale throughout the surface of the concretion.

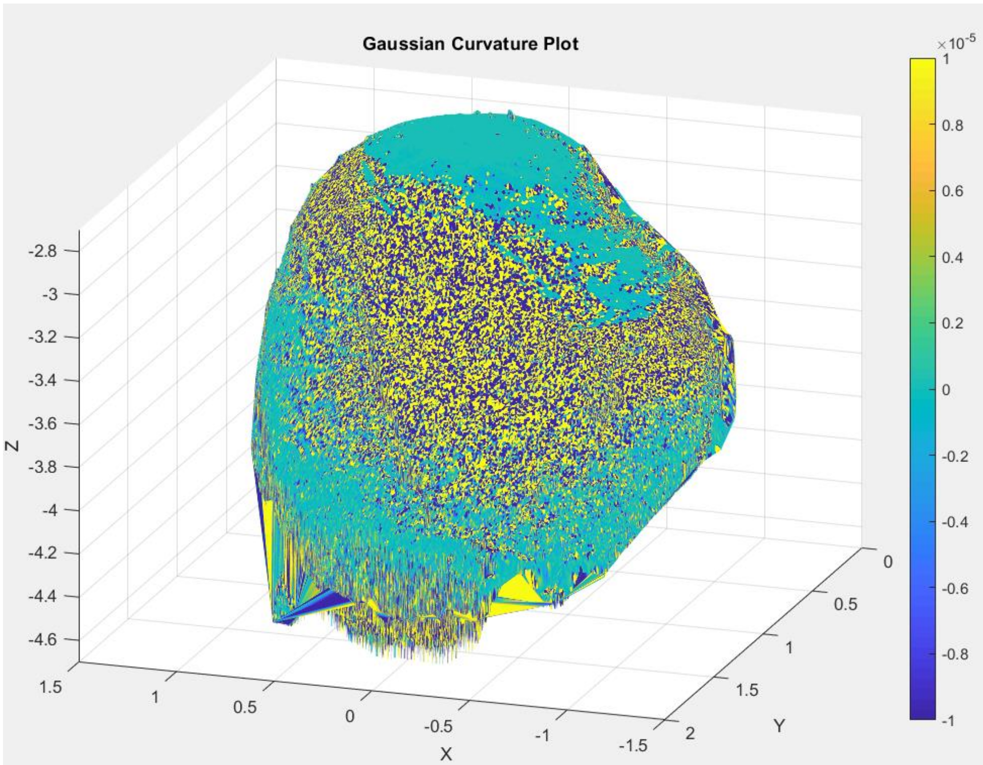

Figure 10: Gaussian curvature plotted by the color scale throughout the surface of the concretion.

Discussion

Field Observations

The first noticeable pattern in the dataset is that there are different patterns between the outer ring fractures and the fractures that pierced all rings. This suggests that there are two sets of fractures, opened in separate events. In addition, those fractures that only penetrate the outer ring appear to share similar directions with the joints in the surrounding shale, suggesting the shale joints and the outer ring fractures were created in the same event. The set of fractures that pierce all rings does not share this pattern and could have been created before the shale had lithified, when it was still relatively ductile. This would seem to support the view that concretions are a syngenetic feature and that they form during compaction of the surrounding mud.

It is currently unknown when the second set of fractures, those that only penetrate the outermost ring, was created, but it must be a secondary feature. As a result of brittle failure in the shale, it must have occurred after a higher degree of compaction. If not after compaction, then late in the process at the very least.

It may possible that the first fracturing event took place during the Late Devonian and is linked to a fold observed at Shale Hollow Park, as seen in Figure 11. Part of the fold is filled in with downlapping beds of grey shale, which suggests that the fold was present at the surface during deposition of the overlying beds. This would suggest that the fold is a syndepositional feature and Late Devonian in age. Given the origin of the Appalachian Basin, it is most likely that the fold is related to Acadian tectonic activity and linked to the first set of fractures. For the shale to have folded, it would need to be able to be ductile, making it likely that the shale had experienced little if any compaction by the time the fold and fracture occurred. This further supports the notion that concretion growth occurred quickly and started shortly after burial.

Figure 11. Photo (top) and diagrammatic sketch (bottom) of syndepositional fold in the Huron Shale Member in Shale Hollow Park. Note downlapping and onlapping shale layers that fill the synformal part of the fold.

Surface Curvature

Based on the models, it would seem as though the fractures that propagated outwards radially could be linked to surface curvature. The middle section of the surface has the lowest curvature and has no such fractures. The areas where they begin to show up have an overall higher curvature than the center and an area with overall higher average curvature has the most radial, outwards propagating cracks in it. However, there is not a pattern that appears to follow any particular fractures, suggesting that there isn't an observable link between surface curvature and fracture propagation.

The Gaussian curvature data contains a high order of variance, and the Gaussian curvature model has drastic variance throughout the central portion of the surface. The order of magnitude ranges from -6 to -28 in some places, which means the overall Gaussian curvature is very small and the wide range makes it harder to plot smoothly. However, the small Gaussian values do precisely show the small bumps and variations in curvature that one would expect to find on a hand sample. Mean curvature seems to be more useful in determining a link between surface shape and fracture propagation, as the high variance in Gaussian curvature can obfuscate features on the surface.

CONCLUSIONS

The objective of this study was to determine whether a link exists between septarian concretion formation and syndepositional tectonic activity. Given the physical proximity between the early phase of septarian development and the presence of syndepositional folding, a correlation seems likely. The timing of fracturing appears to have been during the the time of clay sedimentation, but following initial diagenesis of the concretions. The work done by Borkow and Babcock showed that early mineralization leading to concretion development begins within days of the initial decay of tissues in an organism at the nucleus of a concretion (2001). Having been deposited in the Late Devonian, the Ohio Shale would have been deposited during the Acadian orogeny and it is possible that activity from the Acadian fractured the concretions just after they had formed. Cracks present only in the outer rings of 3-ring septarian concretions have trends equal to the joint directions in the black shale matrix. Those cracks seem to be related and have a later origin. The origin and timing of that fracturing is unknown, but it must have occurred post-lithification.

The timing of the fractures is also a point of interest. There appear to be two sets of fractures. One only observed in the concretions and one observed in both the concretions and the surrounding shale. This would support the interpretation that concretions as a syngenetic feature.

The objective of the 3D model analysis was to determine if there is a correlation between fracture propagation and surface curvature in septarian concretions. The models do not display any patterns that closely follow any of the fractures and don’t seem to support a potential correlation. It is possible that such a correlation exists, but alternative methods should be used in future research.

Recommendations for Future Work

To test the conclusions of this study, one could perform a similar study on septarian concretions in units corresponding to the Ohio Shale. Corresponding units occur from New York to Tennessee and septarian concretions can be found in them as well. If the fractures display similar patterns, that would support the conclusions presented in this study. Additionally, one could analyze the chemical properties of the individual concretion rings. Given one set of fractures only penetrated the outer ring, there may be a difference in composition between rings. Finally, the existence of Late Devonian faults through the area of the unit's occurrence would give a likely candidate for the source of the stress deforming the shale and fracturing the concretions.

References Cited

Borkow, P. S., & Babcock, L. E. (2003). Turning pyrite concretions outside-in: role of biofilms in pyritization of fossils. *The Sedimentary Record*, *1*(3), 4-7.

Hellstrom, L. W., & Babcock, L. E. (2000). High-resolution stratigraphy of the Ohio Shale (upper Devonian), central Ohio. *Northeastern Geology and Environmental Sciences*, *22*(3), 202-226.

Pollard, D., Pollard, D. D., Fletcher, R. C., & Fletcher, R. C. (2005). *Fundamentals of structural geology*. Cambridge University Press.

Appendices

Concretion Fracture Rose Diagrams

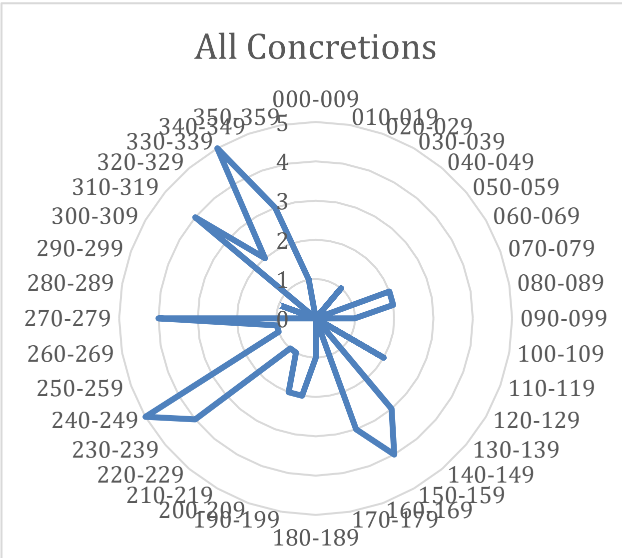

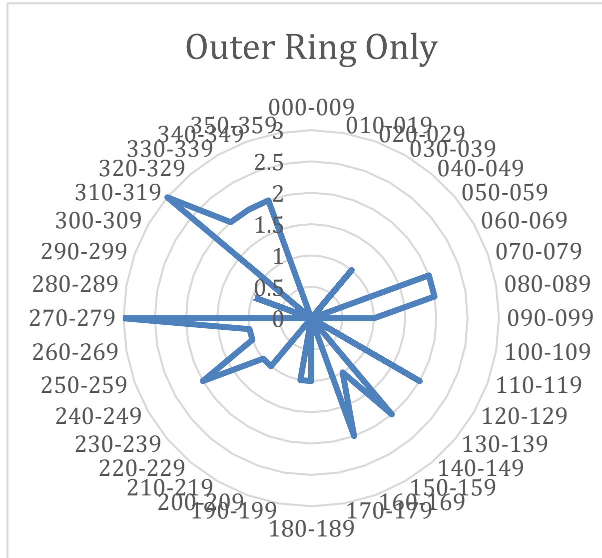

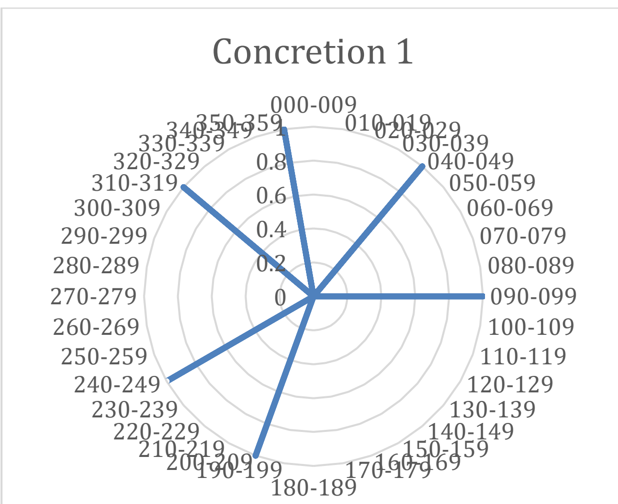

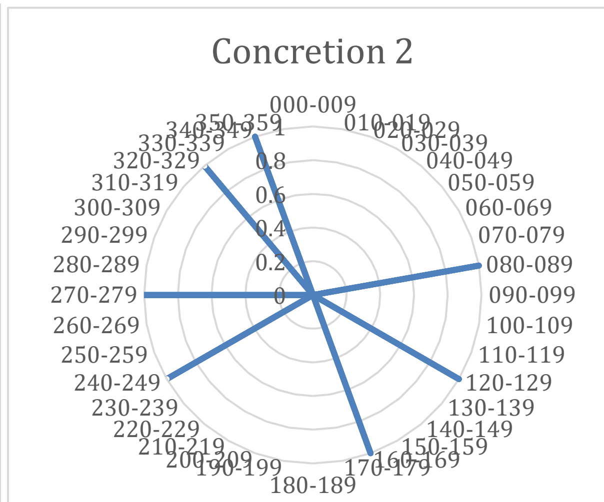

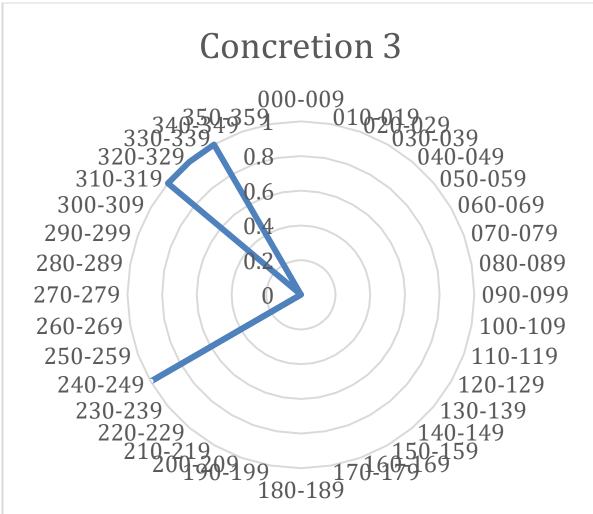
Concretion 3

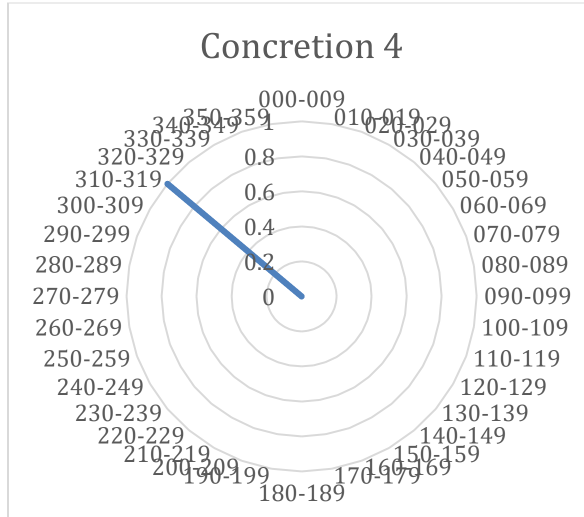
Concretion 4

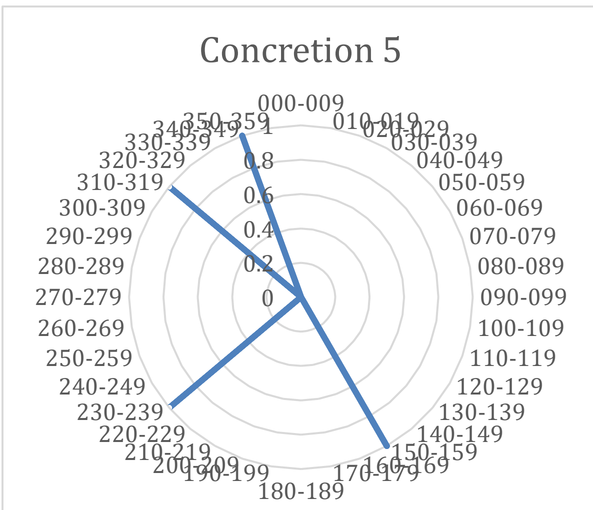
Concretion 5

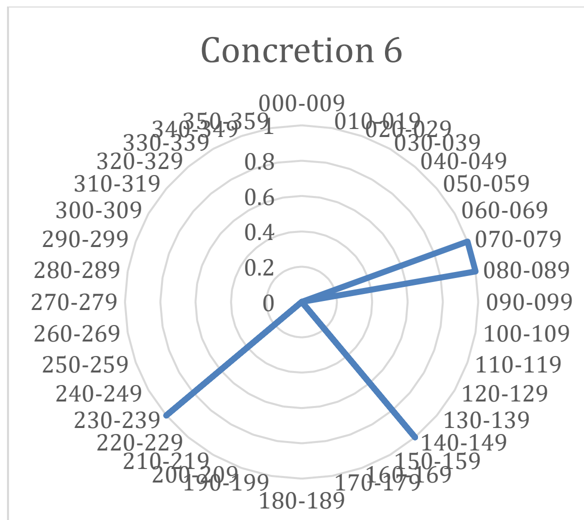
Concretion 6

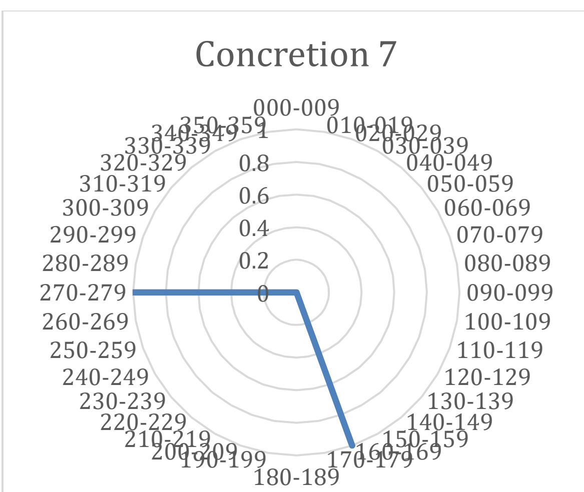
Concretion 7

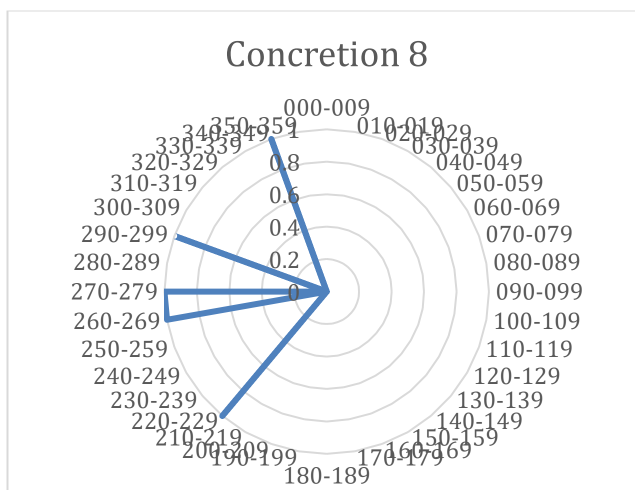
Concretion 8

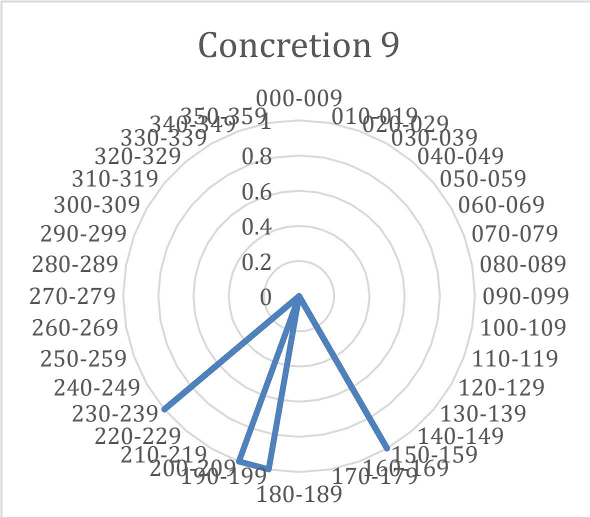
Concretion 9
0
0.2
0.4
0.6
0.8
1
000-009
010-019
020-029
030-039
040-049
050-059
060-069
070-079
080-089
090-099
100-109
110-119
120-129
130-139
140-149
150-159
160-169
170-179
180-189
190-199
200-209
210-219
220-229
230-239
240-249
250-259
260-269
270-279
280-289
290-299
300-309
310-319
320-329
330-339
340-349
350-359

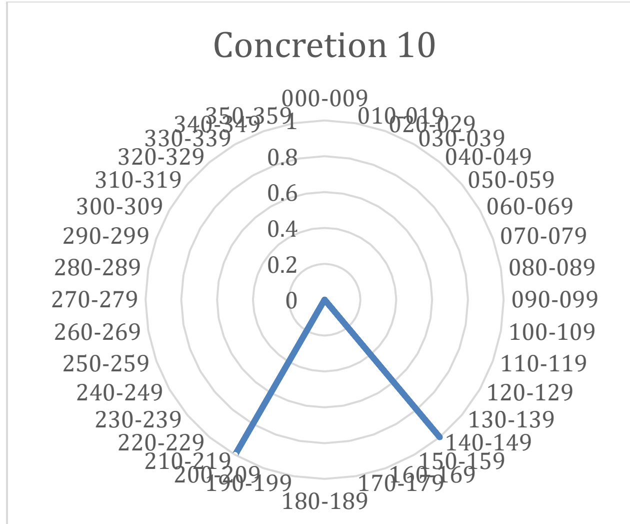
Concretion 10
0
0.2
0.4
0.6
0.8
1
000-009
010-019
020-029
030-039
040-049
050-059
060-069
070-079
080-089
090-099
100-109
110-119
120-129
130-139
140-149
150-159
160-169
170-179
180-189
190-199
200-209
210-219
220-229
230-239
240-249
250-259
260-269
270-279
280-289
290-299
300-309
310-319
320-329
330-339
340-349
350-359

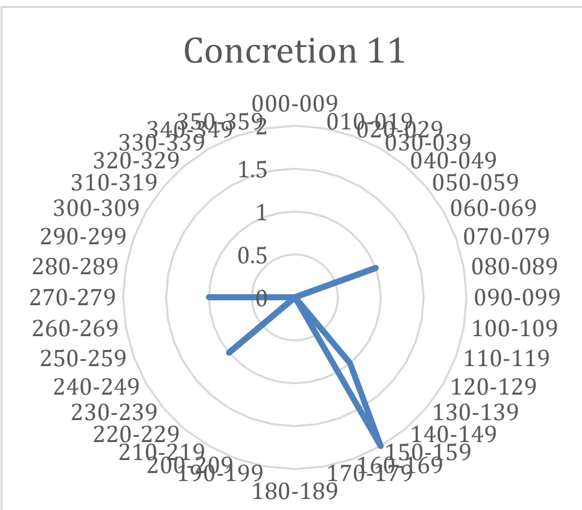
Concretion 11
0
0.5
1
1.5
2
000-009
010-019
020-029
030-039
040-049
050-059
060-069
070-079
080-089
090-099
100-109
110-119
120-129
130-139
140-149
150-159
160-169
170-179
180-189
190-199
200-209
210-219
220-229
230-239
240-249
250-259
260-269
270-279
280-289
290-299
300-309
310-319
320-329
330-339
340-349
350-359

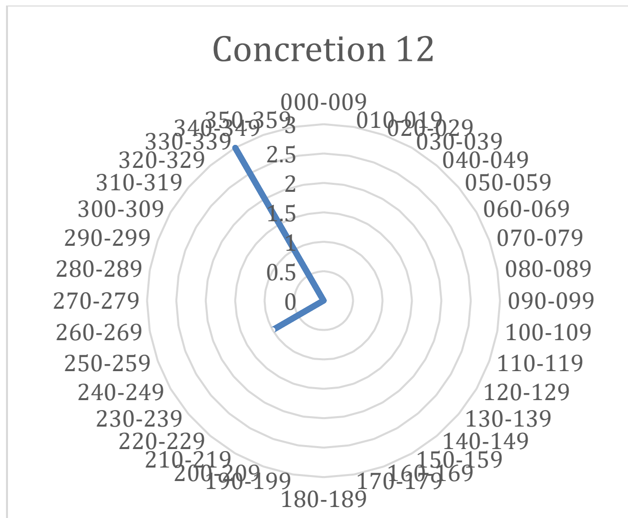
Concretion 12
0
0.5
1
1.5
2
2.5
3
000-009
010-019
020-029
030-039
040-049
050-059
060-069
070-079
080-089
090-099
100-109
110-119
120-129
130-139
140-149
150-159
160-169
170-179
180-189
190-199
200-209
210-219
220-229
230-239
240-249
250-259
260-269
270-279
280-289
290-299
300-309
310-319
320-329
330-339
340-349
350-359

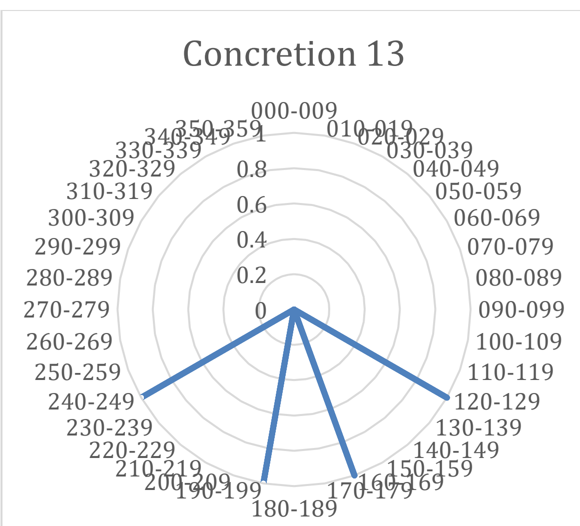
Concretion 13
0
0.2
0.4
0.6
0.8
1
000-009
010-019
020-029
030-039
040-049
050-059
060-069
070-079
080-089
090-099
100-109
110-119
120-129
130-139
140-149
150-159
160-169
170-179
180-189
190-199
200-209
210-219
220-229
230-239
240-249
250-259
260-269
270-279
280-289
290-299
300-309
310-319
320-329
330-339
340-349
350-359

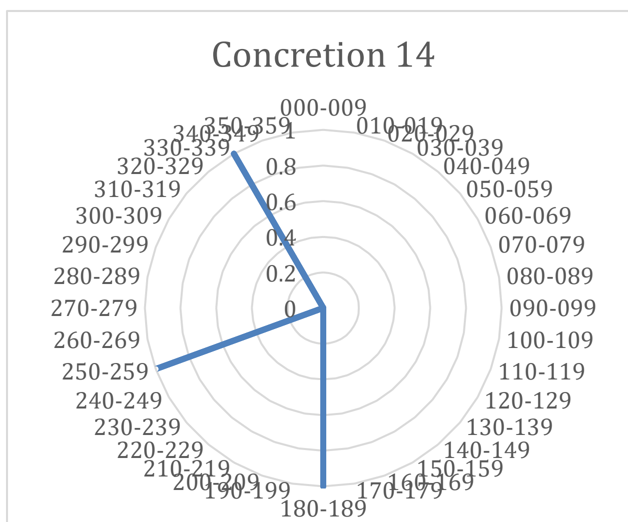
Concretion 14
0
0.2
0.4
0.6
0.8
1
000-009
010-019
020-029
030-039
040-049
050-059
060-069
070-079
080-089
090-099
100-109
110-119
120-129
130-139
140-149
150-159
160-169
170-179
180-189
190-199
200-209
210-219
220-229
230-239
240-249
250-259
260-269
270-279
280-289
290-299
300-309
310-319
320-329
330-339
340-349
350-359

Data Table of Recorded Fracture Directions

Concretion Number	Strike	Rings Penetrated		
		1	2	3
	248			yes
	316	yes	yes	yes
	355		yes	yes
	40			yes
	93			yes
	165		yes	yes
1	204		yes	yes
	348			yes
	325			yes
	276			yes
	245			yes
	160			yes
	125			yes
2 (poorly exposed)	80			yes
	248	yes	yes	N/A
	321		yes	N/A
	337		yes	N/A
3	311		yes	N/A
4	312		yes	N/A
	311		yes	N/A
	348	yes	yes	N/A
	231		yes	N/A
5	158	yes	yes	N/A
	239	yes	yes	N/A
	87		yes	N/A
	144		yes	N/A
6	77		yes	N/A
	270		yes	N/A
7	169	yes	yes	N/A
	225			yes
	263			yes
	274			yes
	297			yes
8 (poorly exposed)	346			yes
	232	yes	yes	yes
9	200		yes	yes

	195		yes	yes
	155			yes
10 (not opened)	212	N/A	N/A	N/A
	147	N/A	N/A	N/A
11	153	yes	yes	yes
	150			yes
	140		yes	yes
	77			yes
	273	yes	yes	yes
	234		yes	yes
12 (used Brunton with 4.5 degree correction)	334	yes	yes	N/A
	334	yes	yes	N/A
	334	yes	yes	N/A
	245	yes	yes	N/A
13 (used Brunton with 4.5 degree correction)	243	yes	yes	N/A
	190		yes	N/A
	125		yes	N/A
	160		yes	N/A
14 (used Brunton with 4.5 degree correction)	180		yes	N/A
	334		yes	N/A
	257		yes	N/A

Shale Joints		
Strike	Dip	Dip Direction
270	67	N
5	84	W
175	75	W
147	88	W
120	67	SW
359	80	E

FractureCurvature.m file

```
clear all, clf reset;
fv = stlread('JacobsConcretion.stl');
[Cmean,Cgaussian,Dir1,Dir2,Lambda1,Lambda2]=patchcurvature(fv,true);
figure(1)
patch(fv,'FaceColor',       [0.8 0.8 1.0], ...
         'EdgeColor',       'none',        ...
         'FaceLighting',    'gouraud',     ...
         'AmbientStrength', 0.15);

% Add a camera light, and tone down the specular highlighting
camlight('headlight');
material('dull');
xlabel('X'), ylabel('Y'), zlabel('Z');
xlim([-1.5 1.5]);
ylim([0 2]);
zlim([-4.7 -2.7]);

% Fix the axes scaling, and set a nice view angle
axis('image');
%%
[F, V] = stlread('JacobsConcretion.stl');
x = V(1:end, 1);
y = V(1:end, 2);
z = V(1:end, 3);
dt = delaunayTriangulation(x,y) ;
tri = dt.ConnectivityList ;
xi = dt.Points(:,1) ;
yi = dt.Points(:,2) ;
F = scatteredInterpolant(x,y,z);
zi = F(xi,yi);
Fc = scatteredInterpolant(x,y,Cmean);
ci = Fc(xi, yi);
figure(2)
trisurf(tri, xi, yi, zi, ci)
xlim([-1.5 1.5]);
ylim([0 2]);
zlim([-4.7 -2.7]);
xlabel('X'), ylabel('Y'), zlabel('Z');
colorbar
shading interp
```